Phase structure of the interacting Su-Schrieffer-Heeger model and the relationship with the Gross-Neveu model on lattice

Yoshihito Kuno
Department of Physics, Graduate School of Science, Kyoto University, Kyoto 606-8502, Japan

(Received 12 November 2018; revised manuscript received 24 January 2019; published 11 February 2019)

The N-flavor interacting Su-Schrieffer-Heeger (i-SSH) model realizable in cold atoms in an optical lattice is studied. We clarify the relationship between the i-SSH model and the Chiral-Gross-Neveu-Wilson (CGNW) model. Following the previous study of the CGNW model in the high-energy physics community, the ground-state phases of the i-SSH model are investigated and interpreted from the viewpoint of the phases of the CGNW model. The interaction effect on the i-SSH model, belonging to the topological BDI class, is grasped by following the view of the dynamical breakdown of chiral symmetry in the CGNW model. Furthermore, we compare the large-N ground-state phase diagram with that of the $N = 1$ case obtained by exact diagonalization, and then we propose a tabletop cold-atom quantum simulator to test the model.

DOI: 10.1103/PhysRevB.99.064105

I. INTRODUCTION

The topological condensed-matter model is deeply related to the high-energy physics model in a lattice. In particular, topological insulators are known to be related to Dirac fermions in a lattice [1,2], which is a major component in high-energy physics in a lattice [3–5]. Investigation of the relationship between the topological condensed-matter model and the high-energy physics model on a lattice leads to a deep understanding of the phases of matter in the topological condensed-matter model. With the help of a high-energy physics study, there is a new possibility to understand the strongly correlated topological model and its novel phase structure. Such interdisciplinary research can give us important insights into strongly correlated topological systems. For example, recently a relationship between a cold-atom condensed-matter model with a nontrivial topological phase and a high-energy physics model has been discussed [6–9]. Such an approach also gives us a deep understanding of the topological condensed-matter model, which is realizable in cold-atom systems. However, an interdisciplinary study of strongly correlated topological systems is still lacking. Thus, in this work, motivated by previous studies [6,10,11], we study a fundamental topological model with interactions, the interacting Su-Schrieffer-Heeger (i-SSH) model [12,13], and we show that the i-SSH model has a clear relationship with the Chiral-Gross-Neveu-Wilson (CGNW) model, which has been extensively studied in the high-energy physics community [10,14,15] because the model has common features of lattice quantum chromodynamics (QCD) [4]. In high-energy physics, the N-flavor CGNW model has been analyzed using the large-N expansion and turned out to possess a rich phase diagram [10]. Following the study, the N-flavor (component) i-SSH model is studied using the large-N expansion. In particular, we study how topological phases are affected by interaction. The i-SSH model exhibits a rich phase diagram induced by interactions. The ground-state phase diagram has a clear correspondence to that of the CGNW model. Furthermore, we investigate the N-flavor dependence of the model, and then we propose implementation schemes to realize the i-SSH model in cold atoms in an optical lattice.

The paper is organized as follows. In Sec. II, our target model is introduced. In Sec. III, we show the relationship between the i-SSH model and the CGNW model. In Sec. IV, we explain the large-N calculation and show the large-N ground-state phase diagram of the i-SSH model. In Sec. V, we carry out an exact diagonalization for the i-SSH model, and we obtain global phase diagrams of the single flavor case of the i-SSH model, and then we compare the result to the large-N result. In Sec. VI, we discuss the implementation scheme of the i-SSH model by using recent cold-atom experimental techniques. Finally, the conclusion is given in Sec. VII.

II. N-FLAVOR SSH MODEL AND CGNW MODEL

We start with the N-flavor Su-Schrieffer-Heeger (SSH) model [12,13],

$$H_S^N = -\sum_i \sum_{\alpha=1}^{N} (J_1 a^\dagger_{\alpha,i} b_{\alpha,i} + J_2 a^\dagger_{\alpha,i+1} b_{\alpha,i} + \text{H.c.}), \tag{1}$$

where $a^{(\dagger)}_{\alpha,i}$ and $b^{(\dagger)}_{\alpha,i}$ are annihilation (creation) operators for the left and right inner site in a unit cell i, α is the flavor index, and $J_{1(2)}$ is the inner (inter) site hopping amplitude. In this work, we consider two types of SU(N) symmetric interactions $V_{\text{I(II)}}$,

$$V_{\text{I}} = -\frac{U}{2N} \sum_i \left[\sum_{\alpha=1}^{N} \left(n^a_{\alpha,i} - n^b_{\alpha,i} \right) \right]^2,$$

$$V_{\text{II}} = V_{\text{I}} - \frac{U}{2N} \sum_i \left[\sum_{\alpha=1}^{N} \left(n^a_{\alpha,i+1} - n^b_{\alpha,i} \right) \right]^2,$$

where $n^{a(b)}_{\alpha,i} = a^\dagger_{\alpha,i} a_{\alpha,i} (b^\dagger_{\alpha,i} b_{\alpha,i})$ is the particle number operator and U is the interaction strength. The above interactions may be realized in a cold-atom experimental system [16–18]. For the $N > 1$ case, though attractive on-site interactions between different flavors and repulsive nearest-neighbor (NN) interactions appear, there is a possibility to tune these interactions by combining recent experimental techniques, e.g., Feshbach and orbital-Feshbach resonance [19,20] and dipole-dipole interaction (DDI) [21,22]. For the case $N = 1$ (single-component case), the situation is quite simple. V_{I} reduces to a repulsive interaction between NN sites in the same unit cell i and V_{II} reduces to a repulsive interaction appearing in all pairs of NN sites. Here, the i-SSH model is defined as $H_S^N + V_{\mathrm{I(II)}}$. In what follows, we call the Hamiltonian $H_S^N + V_{\mathrm{I(II)}}$ the type-I (II) i-SSH model. In the context of condensed system physics, the type-II interaction is related to the z-component Hund's rule coupling in a spin-$N/2$ system [23].

The bulk-momentum Hamiltonian of Eq. (1) for a certain flavor α is given by $h^S_\alpha(k) = [-J_1 - J_2\cos k]\hat{\sigma}_x + [-J_2 \sin k]\hat{\sigma}_y$. Then, using a spinor field $f_\alpha(k) = (a_\alpha(k), b_\alpha(k))^t$, the second quantization form is written as $\sum_{\alpha=1}^N \int \frac{dk}{2\pi} f^\dagger_\alpha(k) h^S_\alpha(k) f_\alpha(k)$. This form is used in the large-N expansion.

Next, we consider the N-flavor CGNW model [6,10,15]. The model is written using Wilson fermions [3,4]. Then, the model includes an additional NN hopping term, called the Wilson term, parametrized by r, called the Wilson parameter [3,4,6,10]. The model is given by

$$
\begin{aligned}
H^N_G = &\sum_i \sum_{\alpha=1}^N \Big[\frac{1}{2}[\bar{\psi}_{\alpha,i}(-i\gamma^1)\psi_{\alpha,i+1} + \mathrm{H.c.}] \\
&+ m_0 \bar{\psi}_{\alpha,i}\psi_{\alpha,i} - \frac{r}{2}(\bar{\psi}_\alpha \psi_{\alpha,i+1} + \mathrm{H.c.})\Big] \\
&- \frac{g^2}{4N}\sum_i \left[\left(\sum_{\alpha=1}^N \bar{\psi}_{\alpha,i}\psi_{\alpha,i}\right)^2 - \left(\sum_{\alpha=1}^N \bar{\psi}_{\alpha,i}\gamma^5\psi_{\alpha,i}\right)^2\right],
\end{aligned}
\tag{2}
$$

where $\psi_{\alpha,i}$ is the spinor field with a flavor α on lattice site i, and the gamma matrices are set as $\gamma^0 = \hat{\sigma}_z$, $\gamma^1 = -i\hat{\sigma}_y$, $\gamma^5 = \hat{\sigma}_x$, and $\bar{\psi}_{\alpha,i} = \psi^\dagger_{\alpha,i}\gamma^0$. m_0 is the effective mass, defined as $m_0 \equiv m + \frac{r}{2}$, where m is the Wilson mass. g^2 is the coupling constant of the interaction that is invariant for continuous chiral symmetry transformation [24].

In this study, we set the lattice spacing to unity and set $r = 1$. Then, the bulk-momentum Hamiltonian of the noninteracting part of H^N_G for a flavor α is given by $h^G_\alpha(k) = [m + 1 - \cos k]\hat{\sigma}_x + [\sin k]\hat{\sigma}_y$. The dispersion of $h^G_\alpha(k)$ with $r \neq 0$ avoids having zero energy at $k = \pm\pi$; thus, the fermion doubler is eliminated [3,4].

III. RELATIONSHIP

There is a clear relationship between the type-I i-SSH model and the CGNW model. The left and right inner sites in a unit cell in the type-I i-SSH model correspond to the color degrees of freedom of the Wilson fermion in the CGNW model. There exists a clear correspondence between the gamma matrices in $h^G_\alpha(k)$ and the Pauli matrices in $h^S_\alpha(k)$: $\gamma^0 \longleftrightarrow \hat{\sigma}_x$, $\gamma^1 \longleftrightarrow -i\hat{\sigma}_z$, and $\gamma^5 \longleftrightarrow \hat{\sigma}_y$. Furthermore, by imitating the form of the interaction in Eq. (2), we can deform V_{I} in the type-I i-SSH model into

$$
V_{\mathrm{I}} = -\frac{U}{4N}\sum_i \left[\left(\sum_{\alpha=1}^N f^\dagger_{\alpha,i}\hat{\sigma}_x f_{\alpha,i}\right)^2 - \left(\sum_{\alpha=1}^N f^\dagger_{\alpha,i} i\hat{\sigma}_z f_{\alpha,i}\right)^2\right],
\tag{3}
$$

where $f_{\alpha,i}$ is a spinor field, $f_{\alpha,i} = (a_{\alpha,i}, b_{\alpha,i})^t$. By comparing Eq. (3) with the form of the interaction in Eq. (2), there are operator relations between the type-I i-SSH model and the CGNW model:

$$
f^\dagger_{\alpha,i}\hat{\sigma}_x f_{\alpha,i} \longleftrightarrow \bar{\psi}_{\alpha,i}\psi_{\alpha,i}, \tag{4}
$$

$$
f^\dagger_{\alpha,i} i\hat{\sigma}_z f_{\alpha,i} \longleftrightarrow \bar{\psi}_{\alpha,i}\gamma^5\psi_{\alpha,i}. \tag{5}
$$

These relations indicate that the inner-bond operator in the i-SSH model corresponds to the particle-antiparticle pairing operator in the CGNW model, and the density-difference operator between the left and right inner site in a unit cell corresponds to the pseudoscalar operator, which corresponds to a pion field and whose expectation value characterizes a pion condensation in the high-energy physics context [4,10,15].

In a high-energy physics study, the CGNW model with $m = 0$ and $r = 0$ has been expected to have a nonzero expectation value of $\bar{\psi}_{\alpha,i}\psi_{\alpha,i}$ due to the interaction g^2, which is known as the spontaneous dynamic breakdown of chiral symmetry [5,15]. Here, because our CGNW model is assumed to have a finite mass $m_0 \neq 0$, the model does not exhibit such a spontaneous chiral symmetry breaking. However, the dynamical effect induced by the interaction g^2 affects the value of the mass term m_0. Then, from the relation of Eq. (4) and by comparing $h^G_\alpha(k)$ with $h^S_\alpha(k)$, we expect that in the i-SSH model, the same mechanism leads to a modification of the parameter J_1, that is, interaction acts as a correction for the parameter J_1, which determines the strength of the inner-bond order in the i-SSH model.

Some previous studies [10,14] have expected that the CGNW model has a novel state with a nonzero expectation value of $\bar{\psi}_{\alpha,i}\gamma^5\psi_{\alpha,i}$ in a large-g^2 regime. This state is known as the Aoki phase, which is a parity-broken phase [5,10,14]. Then, from the relation of Eq. (5), we expect that the Aoki phase corresponds to the density-wave phase in the i-SSH model. In what follows, from a unified perspective, we also call the density-wave order in the i-SSH model the Aoki phase.

The type-II i-SSH model can also be related to the lattice version of an extended Gross-Neveu model, which has nonlocal interactions and has been discussed in a high-energy physics context [25,26]. The V_{II} term can also be deformed in the same way as Eq. (3). The details are explained in the supplemental material [27].

IV. LARGE-N EXPANSION

The large-N expansion has succeeded in capturing the ground-state phase diagram of the CGNW model in high-energy physics [10,14,15]. Motivated by this fact, we apply the large-N expansion to both the type-I and II i-SSH models. According to the classification of the noninteracting topological Hamiltonian [31–33], the SSH model is classified in the

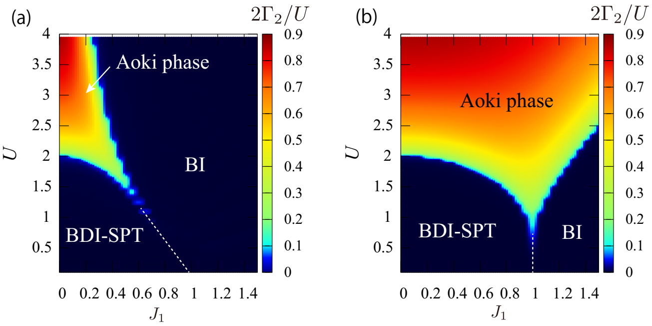

FIG. 1. Large-N phase diagram: (a) type-I i-SSH model, (b) type-II i-SSH model. For both cases, $J_2 = 1$ and three phases appear: the BI phase, the BDI-SPT phase (for odd N case), and the Aoki phase.

BDI class. The Hamiltonian $h^S_\alpha(k)$ has chiral (S), time-reversal (T), and charge-conjugation symmetry (C) [34]. In addition, if an odd N-flavor SSH model is assumed, the model possesses a symmetry-protected topological (SPT) phase [6,35,36].

We investigate how interactions change the topological phase structure of the i-SSH model and break the BDI symmetry. Let us focus on the application of the large-N expansion to the type-I i-SSH model (a detailed treatment is given in the supplemental material [27]). In the large-N expansion, the $V_{\rm I}$ term in the type-I i-SSH model can be decoupled by introducing an auxiliary mean fields $\Gamma_{1(2)}$. These mean fields are introduced in employing the Hubbard-Stratonovich transformation for $V_{\rm I}$ in the process of the large-N calculation when assuming the translational symmetry of the system. Γ_1 and Γ_2 correspond to the expectation values $\langle f^\dagger_{\alpha,i}\hat{\sigma}_x f_{\alpha,i}\rangle$ and $\langle f^\dagger_{\alpha,i} i\hat{\sigma}_z f_{\alpha,i}\rangle$, respectively. Then, Γ_1 and Γ_2 can be incorporated into the Hamiltonian $h^S_\alpha(k)$. The effective bulk-momentum Hamiltonian is given by $h^{\rm I}_\alpha(k) = [-(J_1+\Gamma_1) - J_2\cos k]\hat{\sigma}_x + [-J_2 \sin k]\hat{\sigma}_y + \Gamma_2\hat{\sigma}_z$. Practically, the value of $\Gamma_{1(2)}$ is determined by solving a saddle point equation parametrized by J_1/J_2 and U/J_2 [27]. Here, it is clear that Γ_1 modifies the coupling J_1 as $\tilde{J}_1 = J_1 + \Gamma_1$. If $\Gamma_1 > 0$, Γ_1 acts as an enhancing effect for J_1. Conversely, Γ_2 contributes to the breakdown of BDI symmetry and leads to the Aoki phase. For the Hamiltonian $h^{\rm I}_\alpha(k)$, if $\Gamma_2 \neq 0$, $h^{\rm I}_\alpha(k)$ is no longer in the BDI class because the $\hat{\sigma}_z$ term in $h^{\rm I}_\alpha(k)$ breaks S symmetry. Therefore, if there exists a mean-field solution with $\Gamma_2 \neq 0$, the type-I i-SSH model is not BDI class. This leads the system to not possess a nontrivial topological phase simultaneously with the appearance of the Aoki phase.

By solving numerically the saddle point equation derived from the large-N expansion, we obtain the ground-state phase diagrams for both type-I and type-II i-SSH models, as shown in Fig. 1. For both cases, three phases appear: the band-insulator (BI), the BDI-SPT phase, and the Aoki phase. Here, the phase boundary between the BI and the BDI-SPT phase is determined by $\mathrm{sgn}(\tilde{J}_1 - J_2)$, i.e., if $\tilde{J}_1 > J_2$ ($\tilde{J}_1 < J_2$), the BI (the BDI-SPT) phase appears. The Aoki phase is characterized by $|2\Gamma_2/U| > 0$. The type-I i-SSH phase structure in Fig. 1(a) perfectly corresponds to the phase structure of the previous study for the CGNW model [6]. The BDI-SPT phase is robust up to some extent of interaction strength U. Furthermore, through the value of Γ_1, the $V_{\rm I}$ acts as an enhancing effect for J_1, i.e., the inner-bond order (the BI phase) is enhanced. This appears in the result in Fig. 1(a): The phase boundary line between the BI and the BDI-SPT phase in Fig. 1(a) is not on the line $J_1 = J_2$ with increasing U, but is tilted to the left. For the weak-J_1 regime, the BDI-SPT phase directly transitions to the Aoki phase with increasing U because the Aoki phase is energetically favorable compared with creating the BI phase. Conversely, for the type-II i-SSH model, Fig. 1(b) indicates the enlargement of the Aoki phase compared with the type-I results in Fig. 1(a) and that there is a direct phase transition from the BI to the Aoki phase with increasing U. Also, the BDI-SPT phase is robust up to $U/J_2 \sim 3$. Although the $V_{\rm II}$ acts as a correction effect for both J_1 and J_2 as in the type-I interaction $V_{\rm I}$, this does not change the phase boundary line $J_1 = J_2$ between the BI and the BDI-SPT phase.

The correspondence of the phases between the i-SSH model and the CGNW model is summarized in Table I. Next, we investigate the $N = 1$ case to compare with the large-N result obtained here.

TABLE I. Phase correspondence between the i-SSH model and the CGNW model.

i-SSH model	CGNW model
Band-insulator phase (inner-bond order)	Chirally broken phase (particle-antiparticle pair condensation)
BDI-SPT phase (inter-bond order)	
Density wave phase	Parity-broken Aoki phase (pseudoscalar condensation)

V. $N = 1$ GROUND-STATE PHASE DIAGRAM

Using exact diagonalization, we investigate the ground-state phase diagrams of the type-I and type-II i-SSH models with $N = 1$, where the number of lattice sites is $L = 12$, 16, and 20 with periodic boundary conditions at half-filling, and we employed the Lanczos algorithm [37,38] and finite-size scaling. The obtained phase structures are shown in Fig. 2. Compared with Fig. 1(a), in Fig. 2(a) the phase boundary between the BDI-SPT phase and the Aoki phase rises for the small-J_1 regime. The same behavior has been reported in the CGNW model [6]. In particular, our numerics indicate that

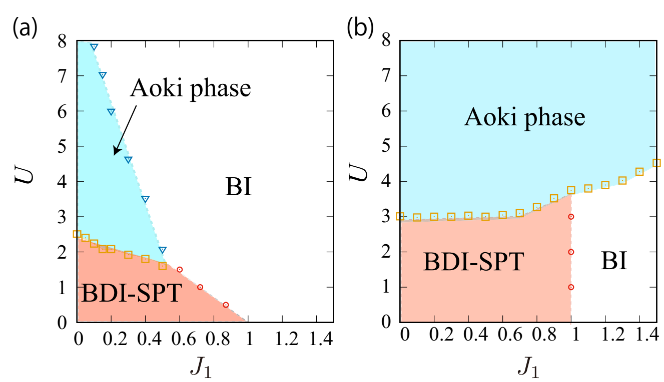

FIG. 2. $N = 1$ phase structures obtained by exact diagonalization: (a) the type-I i-SSH model and (b) the type-II i-SSH model. For both cases, $J_2 = 1$.

the rise at $J_1 = 0$ is smaller than that of the CGNW model case [6]. For Fig. 2(b), the phase boundary of the Aoki phase is lifted as a whole compared with Fig. 1(b). In particular, the tricritical point is lifted compared with Fig. 1(b). We expect that this may be caused by quantum fluctuation effects. However, the details will be studied in future work. The tricritical point in Fig. 2(b) is in agreement with a previous study [36]. After all, we conclude that the $N = 1$ results for the type-I and type-II i-SSH model are in qualitative agreement with the large-N results in Fig. 1. In addition, for Figs. 1(a) and 1(b), the critical behavior toward the Aoki phase is estimated by calculating the order parameter of the Aoki phase $O_{\rm DW}$ and using finite-size scaling [39]. Our numerical calculation indicates that the universality class belongs to the $d = 2$ Ising type, and the critical exponents of $O_{\rm DW}$ take $\beta = 1/8$ and $\nu = 1$; the critical behavior in both type-I and type-II i-SSH models corresponds to the result of the phase transition between the Aoki phase and the BDI-SPT phase in the CGNW model [6]. The details are shown in the supplemental material [27].

VI. IMPLEMENTATION SCHEME FOR COLD-ATOM EXPERIMENTS

There are two types of implementation schemes for the type-I and type-II i-SSH model. In this section, we propose an implementation for the single flavor case $N = 1$. Actually, a recent cold-atom experiment realized the standard SSH model (noninteracting) by using an optical superlattice setup [40], and the SSH model defined on a momentum-space lattice was realized in a cold-atom experiment [41]. Also, Ref. [42] reported the realization of another topological model related to the i-SSH model on a spin-dependent one-dimensional optical lattice.

To realize the type-I i-SSH model in experiments, we employ two different internal states of fermionic atoms, and we prepare two kinds of double-well optical lattice, shown as the blue and green colored lattice potentials in Fig. 3(a). Each double-well optical lattice is fixed on the same one-dimensional spatial axis. Each double-well optical lattice is misaligned by one site with respect to each other, as shown in Fig. 3(a). This system can be feasible using a spin-dependent optical lattice technique [43]. Here, each fermion can be independently trapped for each double-well optical lattice. For this lattice geometry, we add the Rabi coupling Ω by adding an external laser light. The Rabi coupling exchanges the two different internal states of fermions on the same place [44]. The Ω can be regarded as the hopping J_1 in the SSH model. Then, we establish a deep double-well situation for both optical lattices. This situation suppresses the hopping between NN unit cells denoted by $J_{\rm out}$ in Fig. 3(a). The system only remains hopping in a double well, denoted by $J_{\rm in}$ in Fig. 3(a). Then, $J_{\rm in}$ can be regarded as J_2 in the SSH model. Furthermore, in this system, an on-site interaction between the two different internal states of atoms denoted by U_{eg} can be implemented because the two different internal states of fermionic atoms are spatially trapped at the same position. U_{eg} can be regarded as U in the type-I SSH model. Thus, the $V_{\rm I}$ term is realized and we obtain the type-I i-SSH model in this system. Because the type-I i-SSH model is directly connected to the CGNW model, the tabletop experimental simulator of the type-I SSH model has the possibility to become a quantum simulator of the CGNW model.

Conversely, to realize the type-II i-SSH model, a single fermionic atom with a large magnetic dipole moment is suitable. We prepare a one-dimensional double-well optical lattice to trap the atoms. The schematic figure is shown in Fig. 3(b). Here, the lattice geometry directly generates J_1 and J_2 hopping terms in the SSH model. Then, the large magnetic dipole moment of the atom can generate the DDI between NN sites denoted by U_d in Fig. 3(b), corresponding to U in $V_{\rm II}$ if all dipole moments are polarized using external magnetic fields. In real experiments, ^{167}Er [21] and ^{161}Dy [45] degenerate Fermi gasses are candidates to realize the above setup because they have large magnetic dipole moments. A concrete parameter estimation for the two implementation schemes is given in the supplemental material [27]. Our proposed experimental setups cover our target parameter regime for J_1/J_2 and U/J_2, as shown in Figs. 1 and 2.

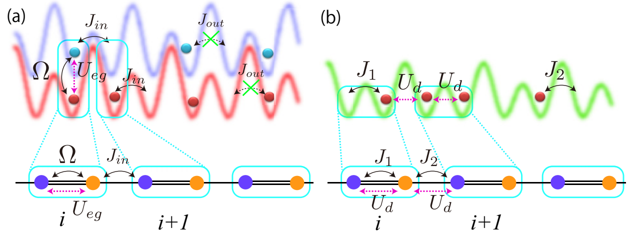

FIG. 3. Implementation scheme using cold atoms in an optical lattice: (a) the type-I i-SSH model, (b) the type-II i-SSH model. In the type-I case, the interaction $V_{\rm I}$ appears as on-site s-wave scattering interaction U_{eg} between the different internal states of fermionic atoms. In the type-II case, the interaction $V_{\rm II}$ is implemented as long-range DDI U_d using a dipolar fermionic atom.

VII. CONCLUSION

We studied an N-flavor i-SSH model and clarified the relationship with the CGNW model. For the i-SSH model, the large-N expansion was carried out. We showed how interaction changes the phase boundary of the BDI-SPT phase and the Aoki phase. The interaction effect appears as a correction for the hopping amplitudes in the SSH model. This mechanism is analogous to the dynamical breakdown of chiral symmetry in the Gross-Neveu model. Furthermore, interactions lead to the breakdown of the S symmetry in the i-SSH Hamiltonian. This makes the i-SSH model out of the BDI class at a certain threshold value U and leads to the Aoki phase. This indicates that the S symmetry breaking is related to the appearance of the Aoki phase. The phase diagram of the i-SSH model with $N = 1$ was also calculated and was compared with the large-N result. The phase diagrams show qualitative agreement with the large-N result. Furthermore, we proposed an implementation scheme to realize the i-SSH model in future experiments.

ACKNOWLEDGMENT

Y.K. acknowledges the support of a Grant-in-Aid for JSPS Fellows (No. 17J00486).

[1] S.-Q. Shen, *Topological Insulators* (Springer-Verlag, Berlin, 2012).

[2] E. Fradkin, *Field Theories of Condensed Matter Physics* (Cambridge University Press, Cambridge, 2013).

[3] K. G. Wilson, *New Phenomena in Subnuclear Physics (Erice, 1975)* (Plenum, New York, 1977).

[4] H. J. Rothe, World Sci. Lect. Notes Phys. **82**, 1 (2012).

[5] M. Creutz, Rev. Mod. Phys. **73**, 119 (2001).

[6] A. Bermudez, E. Tirrito, M. Rizzi, M. Lewenstein, and S. Hands, Ann. Phys. **399**, 149 (2018).

[7] J. I. Cirac, P. Maraner, and J. K. Pachos, Phys. Rev. Lett. **105**, 190403 (2010).

[8] T. V. Zache, F. Hebenstreit, F. Jendrzejewski, M. K. Oberthaler, J. Berges, and P. Hauke, Quantum Sci. Technol. **3**, 034010 (2018).

[9] Y. Kuno, I. Ichinose, and Y. Takahashi, Sci. Rep. **8**, 10699 (2018).

[10] S. Aoki, Phys. Rev. D **30**, 2653 (1984).

[11] Y. Araki and T. Kimura, Phys. Rev. B **87**, 205440 (2013); Y. Araki, T. Kimura, A. Sekine, K. Nomura, and T. Z. Nakano, PoS (**LATTICE 2013**) 050 (2013).

[12] A. J. Heeger, S. Kivelson, J. R. Schrieffer, and W. P. Su, Rev. Mod. Phys. **60**, 781 (1988).

[13] J. K. Asboth, L. Oroszlany, and A. Palyi, *A Short Course on Topological Insulators* (Springer International, New York, 2016), Vol. 919.

[14] M. Creutz, T. Kimura, and T. Misumi, Phys. Rev. D **83**, 094506 (2011).

[15] D. J. Gross and A. Neveu, Phys. Rev. D **10**, 3235 (1974).

[16] M. A. Cazalilla and A. M. Rey, Rep. Prog. Phys. **77**, 124401 (2014).

[17] S. Taie, R. Yamazaki, S. Sugawa, and Y. Takahashi, Nat. Phys. **8**, 825 (2012).

[18] A. V. Gorshkov, M. Hermele, V. Gurarie, C. Xu, P. S. Julienne, J. Ye, P. Zoller, E. Demler, M. D. Lukin, and A. M. Rey, Nat. Phys. **6**, 289 (2010).

[19] S. Inouye, M. R. Andrews, J. Stenger, H.-J. Miesner, D. M. Stamper-Kurn, and W. Ketterle, Nature (London) **392**, 151 (1998).

[20] M. Hofer, L. Riegger, F. Scazza, C. Hofrichter, D. R. Fernandes, M. M. Parish, J. Levinsen, I. Bloch, and S. Folling, Phys. Rev. Lett. **115**, 265302 (2015).

[21] S. Baier, M. J. Mark, D. Petter, K. Aikawa, L. Chomaz, Z. Cai, M. Baranov, P. Zoller, and F. Ferlaino, Science **352**, 201 (2016).

[22] In experiments, the Feshbach resonance technique can make on-site interactions attractive. If one considers a dipolar atom that generates a repulsive NN DDI, the amplitude of the attractive interaction can be tuned to be the same order as that of the DDI.

[23] I. Affleck and F. D. M. Haldane, Phys. Rev. B **36**, 5291 (1987); J. B. Marston and I. Affleck, *ibid.* **39**, 11538 (1989).

[24] The continuous chiral symmetry operation is defined by $\psi_{\alpha,i} \to e^{i\theta\gamma^5}\psi_{\alpha,i}$ and $\bar{\psi}_{\alpha,i} \to \bar{\psi}_{\alpha,i}e^{i\theta\gamma^5}$, where θ is an arbitrary phase parameter.

[25] W. G. Fuertes and J. M. Guilarte, J. Math. Phys. **38**, 6214 (1997).

[26] T. Reisz, Lect. Notes Phys. **508**, 192 (1998).

[27] See Supplemental Material at http://link.aps.org/supplemental/10.1103/PhysRevB.99.064105 for detailed technical aspects, which includes Refs. [28–30].

[28] A. Auerbach, *Interacting Electrons and Quantum Magnetism, Graduate Texts in Contemporary Physics* (Springer New York, 2012).

[29] B. Yang, H. N. Dai, H. Sun, A. Reingruber, Z. S. Yuan, and J. W. Pan, Phys. Rev. A **96**, 011602(R) (2017).

[30] O. Dutta, M. Gajda, P. Hauke, M. Lewenstein, D.-S. Luhmann, B. A. Malomed, T. Sowinski, and J. Zakrzewski, Rep. Prog. Phys. **78**, 066001 (2015).

[31] A. P. Schnyder, S. Ryu, A. Furusaki, and A. W. W. Ludwig, Phys. Rev. B **78**, 195125 (2008).

[32] S. Ryu, A. P. Schnyder, A. Furusaki, and A. W. W. Ludwig, New J. Phys. **12**, 065010 (2010).

[33] A. Kitaev, in *Advances in Theoretical Physics: Landau Memorial Conference*, edited by V. Lebedev and M. Feigel'man, AIP Conf. Proc. No. 1134 (AIP, Melville, NY, 2009), p. 22.

[34] The definition of these symmetries is that a Hamiltonian $H(\mathbf{k})$ possesses the following conditions: for S symmetry $\Gamma H(\mathbf{k})\Gamma^{-1} \neq -H(\mathbf{k})$, for T symmetry $U_T^{-1}H(\mathbf{k})U_T \neq H(-\mathbf{k})$, and for C symmetry $U_C^{-1}H(\mathbf{k})U_C \neq -H(-\mathbf{k})$, where Γ, U_T, and U_C are some symmetry operators and $U_T^2 = +1$ and $U_C^2 = +1$ are satisfied [31]. For $h^S_\alpha(k)$, the operators are given by $\Gamma = \hat{\sigma}_z$, $U_T = K$, and $U_C = \hat{\sigma}_z K$, where K is an imaginary conjugation operator. It is noted that the definition of the S symmetry used here is different from that used in high-energy physics [24].

[35] T. Senthil, Annu. Rev. Condens. Matter Phys. **6**, 299 (2015).

[36] J. Sirker, M. Maiti, N. P. Konstantinidis, and N. Sedlmayr, J. Stat. Mech. (2014) P10032.

[37] P. Prelovsek and J. Bonca, *Strongly Correlated Systems: Numerical Methods* (Springer, Berlin, 2013), Vol. 176.

[38] R. M. Noack and S. R. Manmana, in *Lectures on the Physics of Highly Correlated Electron Systems IX: Ninth Training Course in the Physics of Correlated Electron Systems and High-Tc Superconductors*, edited by A. Avella and F. Mancini, AIP Conf. Proc. No. 789 (AIP, Melville, 2005), p. 93.

[39] In our numerics, the scaling ansatz is $\Psi[(U-U_c)L^{1/\nu}] = L^{\beta/\nu}O_{\rm DW}$, where Ψ is a scaling function and U_c is a transition point, and β and ν are critical exponents. We used the three data sets from different system sizes $L = 12$, 16, and 20.

[40] M. Atala, M. Aidelsburger, J. T. Barreiro, D. Abanin, T. Kitagawa, E. Demler, and I. Bloch, Nat. Phys. **9**, 795 (2013).

[41] E. J. Meier, F. A. An, and B. Gadway, Nat. Commun. **7**, 13986 (2016).

[42] B. Song, L. Zhang, C. He, T. F. J. Poon, E. Hajiyev, S. Zhang, X.-J. Liu, and G.-B. Jo, Sci. Adv. **4**, eaao4748 (2018).

[43] P. Soltan-Panahi, J. Struck, P. Hauke, A. Bick, W. Plenkers, G. Meineke, C. Becker, P. Windpassinger, M. Lewenstein, and K. Sengstock, Nat. Phys. **7**, 434 (2011).

[44] This situation corresponds to a synthetic dimensional technique. For its experimental realization, please refer to M. Mancini *et al.*, Science **349**, 1510 (2015); A. Celi, P. Massignan, J. Ruseckas, N. Goldman, I. B. Spielman, G. Juzeliūnas, and M. Lewenstein, Phys. Rev. Lett. **112**, 043001 (2014).

[45] M. Lu, N. Q. Burdick, and B. L. Lev, Phys. Rev. Lett. **108**, 215301 (2012).